Pictorial Essay | Thoracic Imaging

eISSN 2005-8330
https://doi.org/10.3348/kjr.2019.0181
Korean J Radiol 2019;20(10):1441-1453

Korean Journal of Radiology
KJR

Check for updates

Imaging of Thoracic Wall Abnormalities

Alexandre Semionov, MD[1], John Kosiuk, MD[2], Amr Ajlan, MD[3], Federico Discepola, MD[4]

[1]Department of Diagnostic Radiology, McGill University Health Centre, Montreal General Hospital, Montreal, Canada; [2]Department of Diagnostic Radiology, McGill University Health Centre, Montreal, Canada; [3]Department of Radiology, King Abdulaziz University, Faculty of Medicine, Jeddah, Saudi Arabia; [4]Department of Radiology, Jewish General Hospital, Montreal, Canada

Identification of certain abnormalities of the chest wall can be extremely helpful in correctly diagnosing a number of syndromic conditions and systemic diseases. Additionally, chest wall abnormalities may sometimes constitute diagnoses by themselves. In the present pictorial essay, we review a number of such conditions and provide illustrative cases that were retrospectively identified from our clinical imaging database. These include pentalogy of Cantrell, Klippel-Feil syndrome, cleidocranial dysplasia, Poland syndrome, osteopetrosis, neurofibromatosis type 1, Marfan syndrome, Gardner syndrome, systemic sclerosis, relapsing polychondritis, polymyositis/dermatomyositis, ankylosing spondylitis, hyperparathyroidism, rickets, sickle cell anemia, thalassemia, tuberculosis, septic arthritis of the sternoclavicular joint, elastofibroma dorsi, and sternal dehiscence.
Keyword: *Chest wall abnormalities*

INTRODUCTION

The chest wall is commonly defined as a protective structure around vital organs between the neck and the abdomen and is composed of the skin, subcutaneous fat, muscles, and bones. The latter include ribs and the sternum, spine, and shoulder girdles. The chest wall can be readily assessed by conventional radiography, computed tomography (CT), magnetic resonance imaging (MRI), and nuclear medicine studies. Each of these modalities has its own advantages and specific indications—radiography is readily available and cheap, CT provides superior resolution of bone structures, MRI offers more detailed assessment of the soft tissues, and nuclear medicine allows for detection of metabolically active lesions. A number of syndromic conditions and systemic diseases can affect the chest wall. In certain cases, recognition of characteristic chest wall abnormalities can provide clues to the underlying disease and thus aid in establishing the correct diagnosis. Tables 1 and 2 provide a summary of several such conditions, which are discussed and illustrated below.

Received March 11, 2019; accepted after revision June 10, 2019.
Corresponding author: Alexandre Semionov, MD, Department of Diagnostic Radiology, McGill University Health Centre, Montreal General Hospital, 1650 Cedar Avenue Montreal, Quebec H3G 1A4, Canada.
• Tel: (1514) 934-1934 • Fax: (1514) 934-8263
• E-mail: alexandre.semionov@mail.mcgill.ca

Congenital Diseases

Pentalogy of Cantrell

The hallmark of this syndrome is an omphalocele associated with ectopia cordis. The complete spectrum of the pentalogy consists of deficiency of the anterior diaphragm, midline supraumbilical abdominal wall defect, defect in the diaphragmatic pericardium, congenital intracardiac abnormalities, and defects of the sternum (1). However, only a few patients with the full spectrum of the pentalogy have been described. Anterior body wall defects usually include complete or partial absence of the sternum (Fig. 1). Extrathoracic anomalies may include cleft lip or palate, encephalocele, hydrocephalus, gallbladder agenesis, and polysplenia (1).

Klippel-Feil Syndrome

Klippel-Feil syndrome (KFS) is characterized by congenital fusion of two or more cervical vertebrae. The classical clinical findings of KFS are a short neck, low posterior hairline, and reduced range of cervical motion (2). However, less than half of all individuals with KFS

Table 1. Most Common Imaging Findings of Selected Congenital Pathologies with Chest Wall Involvement

	Chest Wall Findings	Additional Imaging Findings
Pentalogy of Cantrell	Defect in lower sternum or absent sternum	Deficiency of anterior diaphragm. Defect in diaphragmatic pericardium. Ectopia cordis. VSD. ASD. TOF
Klippel-Feil syndrome	Absent or deformed ribs. Fusion of 2 or more vertebrae. Scoliosis. Vertebral instability, Sprengel deformity–elevated scapula. Omovertebral bone	Spina bifida occulta. Congenital heart defects
Cleidocranial dysplasia	Hypoplastic or absent clavicles. Bell-shaped ribcage. Supernumerary ribs	Multiple wormian bones. Brachycephaly. Supernumerary teeth. Basilar invagination. Multiple hemivertebrae. Hypoplastic iliac bones. Hypoplastic or absent fibula and radius
Poland syndrome	Unilateral absence of pectoralis muscles. Absent or hypoplastic ipsilateral ribs, breast and nipple	Ipsilateral syndactyly
Osteopetrosis	Abnormally dense ribs, shoulder girdles and spine. "Sandwich" vertebrae	Generalized abnormally increased bone density, resulting in "bone in bone" appearance
Neurofibromatosis type 1	Cutaneous neurofibromas. Scoliosis, posterior vertebral scalloping, enlarged neural foramina. "Ribbon" ribs. Rib notching. Lateral and anterior meningoceles	Plexiform neurofibromas–mediastinal or pleural masses. Bowing and pseudoarthrosis of long bones
Marfan syndrome	Scoliosis. Pectus excavatum or pectus carinatum. Dural ectasia	Annuloaortic ectasia. Aortic valve insufficiency. Aortic aneurysm. Aortic dissection. Mitral valve prolapse. Pulmonary artery dilatation
Gardner syndrome	Multiple or recurrent desmoid tumours of chest wall	Colonic adenomatous polyps or adenocarcinoma. Gastric and small bowel polyps. Duodenal carcinoma. Thyroid cancer. Osteomas. Dental abnormalities. Epidermoid cysts

ASD = atrial septal defect, TOF = tetralogy of Fallot, VSD = ventricular septal defect

have all three features. One of the commonly encountered features of KFS is the Sprengel deformity, which appears as an elevated scapula on chest radiographs (Fig. 2). The Sprengel deformity is occasionally concomitant with an abnormal omovertebral bone that runs from the cervical or dorsal spine to the scapula. Other anomalies reported in association with KFS include scoliosis, spina bifida occulta, absent or deformed ribs, and congenital heart defects (2).

Cleidocranial Dysplasia

Cleidocranial dysplasia (CCD) is an autosomal dominant skeletal dysplasia characterized by incomplete intramembranous ossification of the bones (3). The thoracic manifestations of CCD include hypoplastic or absent clavicles, a narrow, bell-shaped ribcage, multiple hemivertebrae, and, occasionally, supernumerary ribs (Fig. 3). The extrathoracic findings can include multiple Wormian bones, brachycephaly, supernumerary teeth, basilar invagination, hypoplastic iliac bones, and hypoplastic or absent fibula and radius (3).

Poland Syndrome

Poland syndrome is a rare sporadic condition characterized by congenital unilateral absence of the pectoralis muscles. It may also be associated with absent or hypoplastic ipsilateral ribs, breast and nipple, and ipsilateral syndactyly (4). On chest radiography, Poland syndrome manifests as a hyperlucent hemithorax caused by asymmetry of the chest wall (Fig. 4A). Cross-sectional imaging can demonstrate hypoplasia or aplasia of the pectoral muscles (Fig. 4B) and/or of the breast and ribs.

Osteopetrosis

Osteopetrosis (OP) refers to a group of hereditary diseases characterized by the failure of osteoclasts to resorb bone. As a consequence, bone remodeling is impaired. This results in abnormally dense but fragile bones. In addition to pathological fractures, OP can result in hematopoietic insufficiency, hypocalcemia, disturbed tooth eruption, nerve entrapment syndromes, and growth impairment (5). Radiographs in OP patients that include the spine will

https://doi.org/10.3348/kjr.2019.0181

Korean Journal of Radiology
KJR

Table 2. Most Common Imaging Findings of Selected Acquired Pathologies with Chest Wall Involvement

	Chest wall Findings	Additional Imaging Findings
Collagen vascular diseases		
Systemic sclerosis	Subcutaneous dystrophic calcifications, commonly around SCJs and shoulders	Esophageal dilatation. NSIP or UIP. Flexion deformities and soft tissue atrophy of hands. Acroosteolysis
Relapsing polychondritis	Thickening of costal cartilages. Non-erosive arthropathy of spine	Tracheal stenosis. Tracheal wall thickening and calcification with sparing of posterior membrane. Non-erosive arthropathy of appendicular skeleton
Polymyositis/dermatomyositis	Fatty atrophy of involved muscles. Dystrophic calcifications in muscles and soft tissues	Diaphragmatic elevation/basilar atelectasis. Aspiration pneumonia. NSIP. COP
Spondyloarthropathies		
Ankylosing spondylitis	Syndesmophytes. Enthesitis of interspinal ligaments. Ankylosis of facet, costovertebral and costotransverse joints. Chance-type insufficiency fractures	Upper lobes fibro-bullous disease. Apical fibrosis. Ankylosis of SIJs
Metabolic, storage, and deposition diseases		
Hyperparathyroidism	Resorption of distal clavicles. "Rugger-jersey" spine	Bone resorption. Osteopenia. Brown tumors. Soft tissue calcifications
Rickets	"Rachitic rosary"–nodular enlargement of costochondral junctions	Widening of growth plates. Metaphyseal flaring, cupping and fraying. Osteopenia. Bone deformities. Insufficiency fractures
Hematogenous disorders		
Sickle cell anemia	H-shaped vertebrae. Avascular necrosis of humeral heads	Cardiomegaly. Cephalization of pulmonary vessels. Acute chest syndrome–waxing and waning airspace opacities and pleural effusions. Extramedullary hematopoiesis
Thalassemia	Expansion and coarsened trabeculations of ribs and vertebrae. Low T1 signal intensity of bone marrow	Extramedullary hematopoiesis
Infectious		
TB	Pott's disease–TB spondylodiscitis, paravertebral abscess; may progress to vertebral collapse, kyphosis, gibbus formation. Costal osteomyelitis	Lymphadenopathy. Calcified granulomata. Cavitary lesions, nodules, consolidations. Pleural effusion/empyema. Scarring/chronic atelectasis
Septic arthritis of SCJ	SCJ effusion, widening of joint space, cortical irregularities. May progress to osteomyelitis of proximal clavicle and manubrium with bone erosions or sclerosis. Chest wall abscess/phlegmon and mediastinitis	
Miscellaneous		
Elastofibroma dorsi	Poorly defined, inhomogeneous soft-tissue lesions between chest wall and inferior scapular tip, with density on CT and MRI signal similar to that of skeletal muscle. Often bilateral	
Sternal dehiscence	Progressive post-operative displacement, rotation or fracture of sternal wires. Occasionally lucent strip of more than 3 mm wide along sternotomy. CT may show signs of sternal osteomyelitis and/or mediastinitis	

COP = cryptogenic organizing pneumonia, NSIP = non-specific interstitial pneumonia, SCJ = sternoclavicular joint, SIJ = sacroiliac joint, TB = tuberculosis, UIP = usual interstitial pneumonia

feature characteristic "sandwich vertebrae," resulting from dense bands of sclerosis parallel to the endplates (Fig. 5). Another characteristic radiographic abnormality in OP is the "bone-in-bone" sign, in which abnormal bones appear to have small replicas of themselves inside their normal outline.

Neurofibromatosis Type 1

Neurofibromatosis type 1 (NF1) is the most common of the phakomatoses and results in a variety of manifestations

 https://doi.org/10.3348/kjr.2019.0181

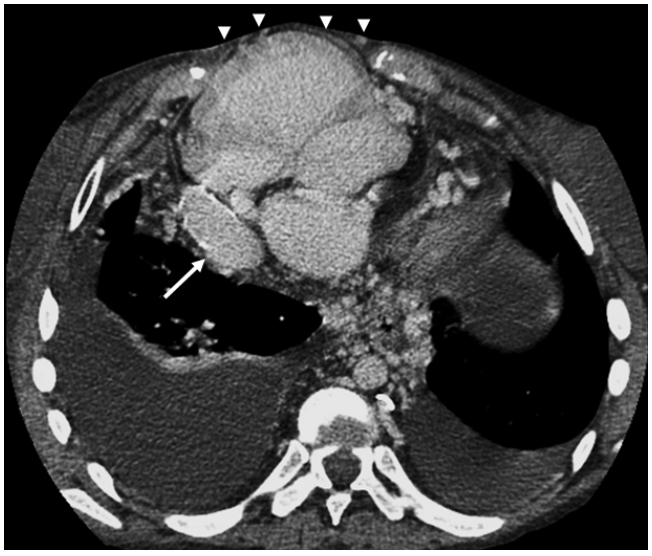

Fig. 1. Pentalogy of Cantrell. Chest CT scan of 25-year-old male with Pentalogy of Cantrell, status post remote Fontan procedure for complex congenital heart abnormality, shows absence of sternum resulting in partial herniation of right ventricle (arrowheads). Note extracardiac Fontan conduit (arrow), multiple mediastinal collateral vessels, and bilateral pleural effusions.

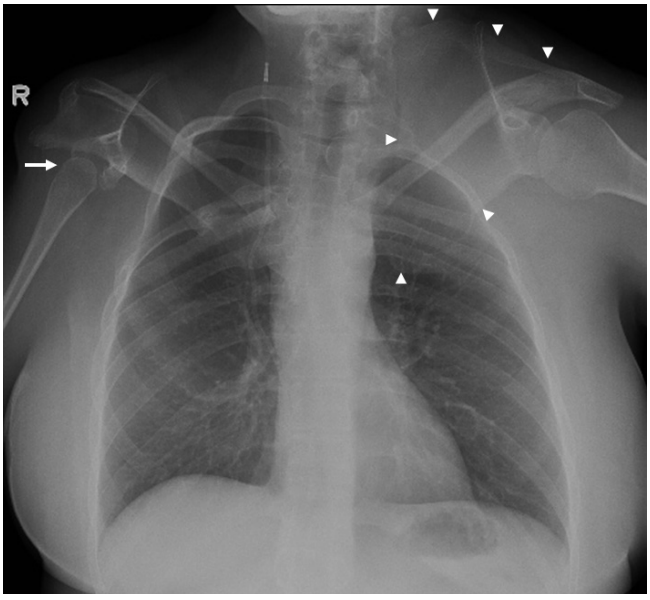

Fig. 2. Klippel-Feil syndrome. Chest radiograph of 39-year-old female with Klippel-Feil syndrome shows hypoplastic right humeral head (arrow), dysmorphic right scapula and glenoid, high-riding left scapula–Sprengel deformity (arrowheads), and multiple upper rib deformities. There is right ventriculo-peritoneal shunt.

throughout the body. NF1 is inherited as an autosomal dominant disorder, but up to half of the cases are caused by spontaneous mutations (6). The classic neurogenic tumors of NF1 are plexiform neurofibromas, which arise from Schwann cells and fibroblasts and may affect any peripheral nerve. Neurofibromas may involve the mediastinum

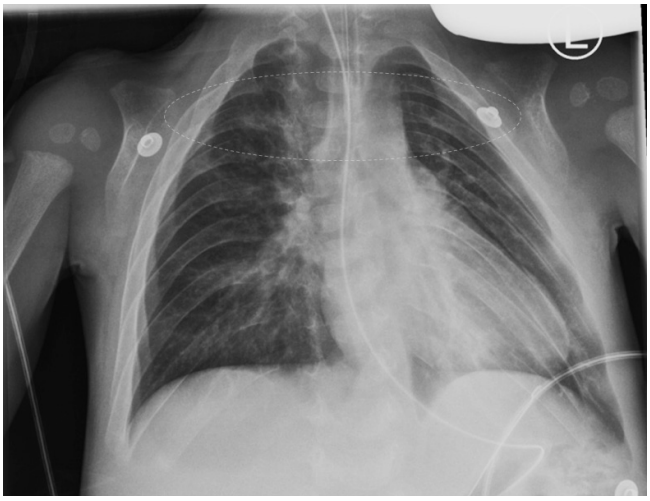

Fig. 3. Cleidocranial dysplasia. Chest radiograph of 3-year-old male with cleidocranial dysplasia shows absence of both clavicles and slanting of ribs. Expected location of clavicles is outlined by dashed line.

and extrapleural space extensively and appear as well-marginated, smooth masses in the paravertebral regions or along the course of the vagus, phrenic, or intercostal nerves (6). Classic CT findings in NF1 with thoracic involvement include small subcutaneous nodules (neurofibromas), thoracic scoliosis, posterior vertebral scalloping, enlarged neural foramina, abnormally thinned ribs–"ribbon-ribs," and rib notching (Figs. 6, 7).

Marfan Syndrome

Marfan syndrome is an autosomal dominant inherited disorder resulting from various mutations of the fibrillin-1 gene, which causes multisystemic connective tissue abnormalities. Up to a third of the cases are sporadic. The cardiovascular and musculoskeletal (MSK) systems are most commonly involved. Potential cardiovascular manifestations include annuloaortic ectasia, aortic aneurysm, aortic dissection, mitral valve prolapse, and pulmonary artery dilatation (7). Thoracic MSK manifestations include scoliosis, pectus excavatum or pectus carinatum, and dural ectasia (Fig. 8).

Gardner Syndrome

Gardner syndrome (GS) is an autosomal dominant colonic polyposis associated with mutations arising in the adenomatous polyposis coli gene, with approximately 20% of patients demonstrating *de novo* mutations (8). GS demonstrates invariable malignant transformation of colonic adenomatous polyps into adenocarcinoma, along with high rates of desmoid tumors and thyroid cancer. Other

https://doi.org/10.3348/kjr.2019.0181

Korean Journal of Radiology
KJR

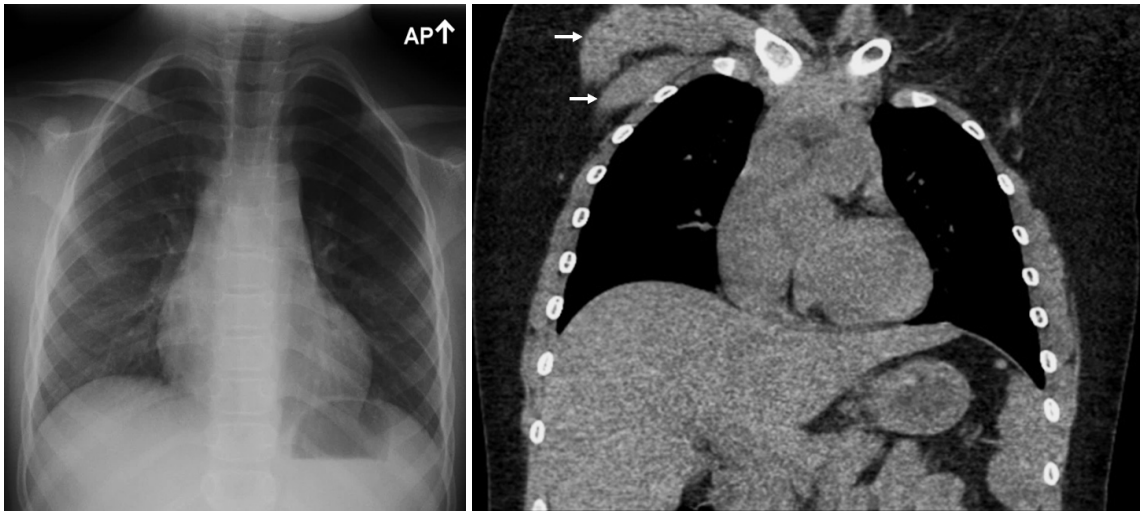

A B

Fig. 4. Poland syndrome. 10-year-old female with Poland syndrome.
A. Chest radiograph demonstrates hyperlucent left hemithorax. **B.** Chest CT with coronal reformation shows absence of left pectoral muscles. Note normal right pectoral muscles (arrows).

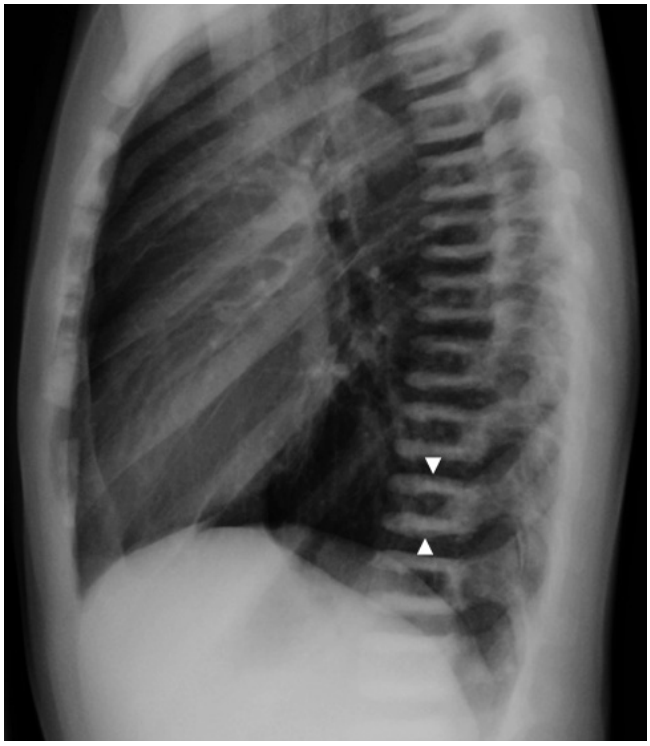

Fig. 5. Osteopetrosis. Lateral chest radiograph of 14-year-old male with osteopetrosis shows abnormally increased density of all bones and characteristic "sandwich vertebrae" (arrowheads).

manifestations of GS include gastric and small bowel polyps, duodenal carcinoma, osteomas, dental abnormalities, retinal pigmentation anomalies, and epidermoid cysts. Multiple or recurrent desmoid tumors of the body wall should alert clinicians to the possibility of GS (Fig. 9).

Fig. 6. Neurofibromatosis type 1. Chest CT scan of 50-year-old female with neurofibromatosis type 1 demonstrates multiple cutaneous neurofibromas (arrowheads).

Acquired Conditions

Systemic Sclerosis

Systemic sclerosis (SS), also known as scleroderma, is a chronic multisystem autoimmune disease of connective tissue associated with vasculopathy. It is characterized by diffuse fibrosis of skin and various internal organs and tissues. SS can manifest with subcutaneous calcinosis, Raynaud's phenomenon, esophageal dysmotility, sclerodactyly, and telangiectasis (9). Interstitial lung disease of non-specific interstitial pneumonia (NSIP) type and pulmonary arterial hypertension are common in patients with SS. Aspiration pneumonia occurs frequently due to esophageal dysfunction. Subcutaneous dystrophic

https://doi.org/10.3348/kjr.2019.0181

calcifications are frequent and are most commonly seen in the fingers, but may occur in any location (Fig. 10).

Relapsing Polychondritis

Relapsing polychondritis (RP) is a rare disease characterized by recurrent inflammation of cartilaginous structures throughout the body, including the auricular, nasal, and laryngeal cartilages, tracheobronchial tree, heart valves, rib cage, and joints of the appendicular skeleton. Airway involvement is seen in half of the patients with RP, and manifests radiologically as subglottic and tracheal stenosis, tracheal wall thickening, and calcification (10), with characteristic sparing of the posterior tracheal membrane (Fig. 11). MSK manifestations of RP include non-erosive arthropathy of the appendicular skeleton, spine, and sacroiliac joints (10). Thickening of the costal cartilages can be seen (Fig. 11).

Fig. 7. Neurofibromatosis type 1. Chest CT with coronal reformation in 16-year-old female with neurofibromatosis type 1 demonstrates multiple rib deformities and bilateral intercostal plexiform neurofibromas (arrows).

Ankylosing Spondylitis

Ankylosing spondylitis (AS) is a multisystem disorder

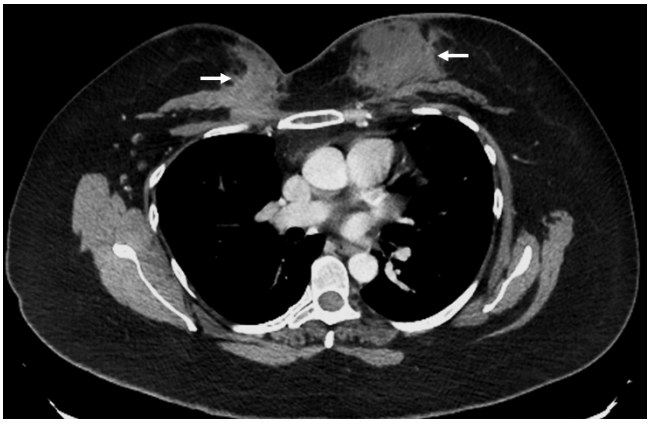

Fig. 9. Gardner syndrome. Chest CT scan of 35-year-old female patient with Gardner syndrome demonstrates bilateral anterior chest wall lesions (arrows), which are biopsy-proven desmoid tumors.

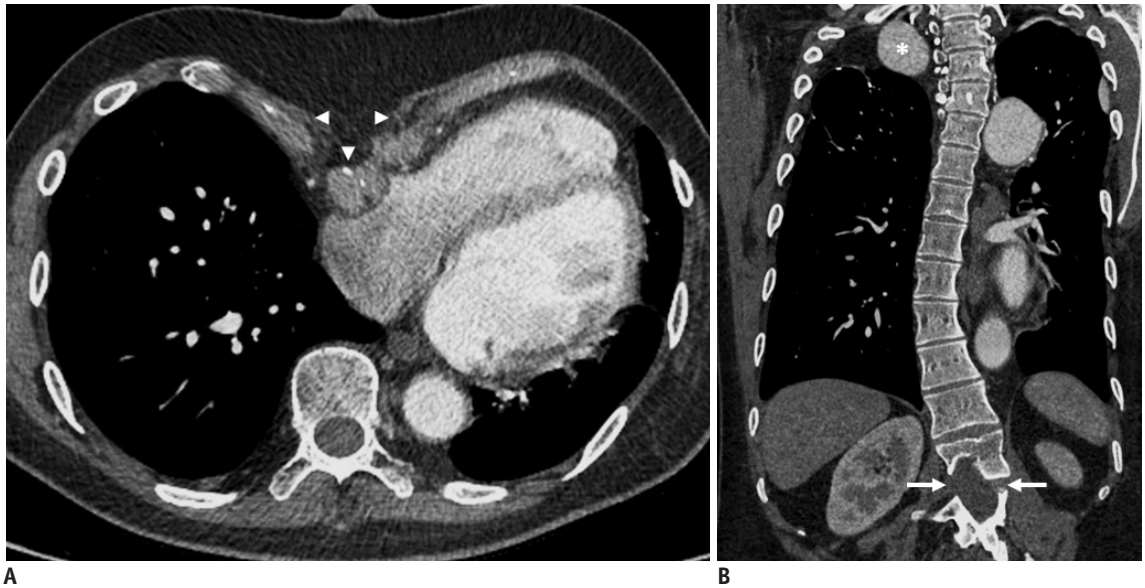

A **B**

Fig. 8. Marfan syndrome.
Axial CT angiogram **(A)** and CT with coronal reformation **(B)** of 25-year-old male with Marfan syndrome show pectus excavatum (arrowheads), scoliosis, upper lumbar dural ectasia (arrows), and aneurysm of right subclavian artery (asterisk).

https://doi.org/10.3348/kjr.2019.0181

Korean Journal of Radiology
KJR

of unknown pathogenesis that primarily affects the joints of the axial skeleton. It is classified as a seronegative spondyloarthritis, and the majority of AS patients are human leukocyte antigen B27 (HLA-B27)-positive (9). AS most commonly manifests as bilateral sacroiliitis and spondylitis, which usually progresses from the lumbosacral to the cervical spine. The characteristic imaging findings of AS include anterior spondylitis, diskitis, syndesmophytes, enthesitis of the interspinal ligaments, marked ankylosis of the sacro-iliac joints, dorsal spine facet joints,

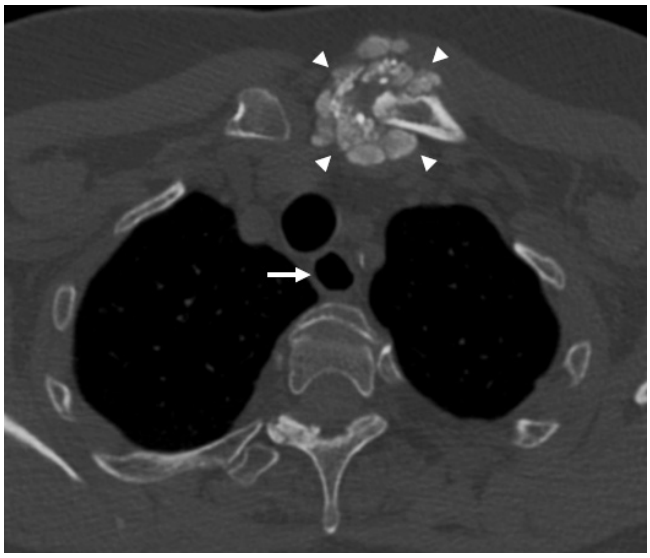

Fig. 10. Systemic sclerosis. Chest CT scan of 54-year-old female with systemic sclerosis shows exuberant amorphous calcifications around left sternoclavicular joint (arrowheads) and patulous esophagus (arrow).

Fig. 11. Relapsing polychondritis. Chest CT scan of 77-year-old male with relapsing polychondritis demonstrates marked thickening of costal cartilages (arrows), as well as thickening of tracheal wall (arrowheads) with sparing of posterior membrane and tracheal luminal narrowing.

A B

Fig. 12. Ankylosing spondylitis.
A. CT with sagittal reformation in 76-year-old male with ankylosing spondylitis shows diffuse ankylosis of thoracolumbar spine. **B.** Chest CT with sagittal reformation in different patient with ankylosing spondylitis shows acute Chance fracture in upper lumbar spine (arrow).

https://doi.org/10.3348/kjr.2019.0181

costovertebral and costotransverse joints, and insufficiency fractures (Fig. 12). Insufficiency fractures of AS are typically of the Chance-type, involving the three columns and running either through the disc space or the juxta-articular endplate (Fig. 12B) (11).

Polymyositis/Dermatomyositis

Polymyositis/dermatomyositis (PM/DM) are idiopathic inflammatory myopathies that manifest as muscle weakness and inflammation. DM is distinguished from PM by the presence of cutaneous manifestations (9). The most common chest findings in PM/DM are diaphragmatic elevation and basilar atelectasis due to diaphragmatic weakness, and aspiration pneumonia due to pharyngeal muscle weakness. Interstitial lung disease is seen in up to one third of patients with PM/DM, NSIP and cryptogenic organizing pneumonia being the most frequently encountered patterns. Longstanding disease might result in fatty atrophy of the involved muscles (Fig. 13). Another typical MSK finding on imaging of patients with PM/DM is dystrophic calcification in the muscles and soft tissues, which is classically sheet-like, the so-called "calcinosis universalis" (Fig. 13).

Fig. 13. Dermatomyositis. Chest CT scan of 51-year-old female with severe dermatomyositis shows diffuse atrophy of chest wall muscles and extensive subcutaneous calcifications in upper arms (arrows).

Hyperparathyroidism

Hyperparathyroidism (HPT) can be primary, secondary, or tertiary. Primary HPT is caused by parathyroid adenoma, hyperplasia, or carcinoma. Secondary HPT is a compensatory mechanism for hypocalcemia that may result from vitamin D deficiency, renal insufficiency, or calcium deprivation. Tertiary HPT occurs secondary to the development of autonomous parathyroid hyperplasia after longstanding secondary HPT. The skeletal changes in primary and secondary HPT are identical. The classical radiographic features of HPT are bone resorption, generalized osteopenia, brown tumors, and soft-tissue calcifications (12). Classical findings of HPT on chest radiography include a "rugger-jersey" spine and bilateral distal clavicular subperiosteal bone resorption (Fig. 14).

Rickets

Rickets refers to osteomalacia caused by failure of osteoid calcification in a growing child and usually occurs as a result of vitamin D deficiency. The classical thoracic manifestation of the disease is the so-called

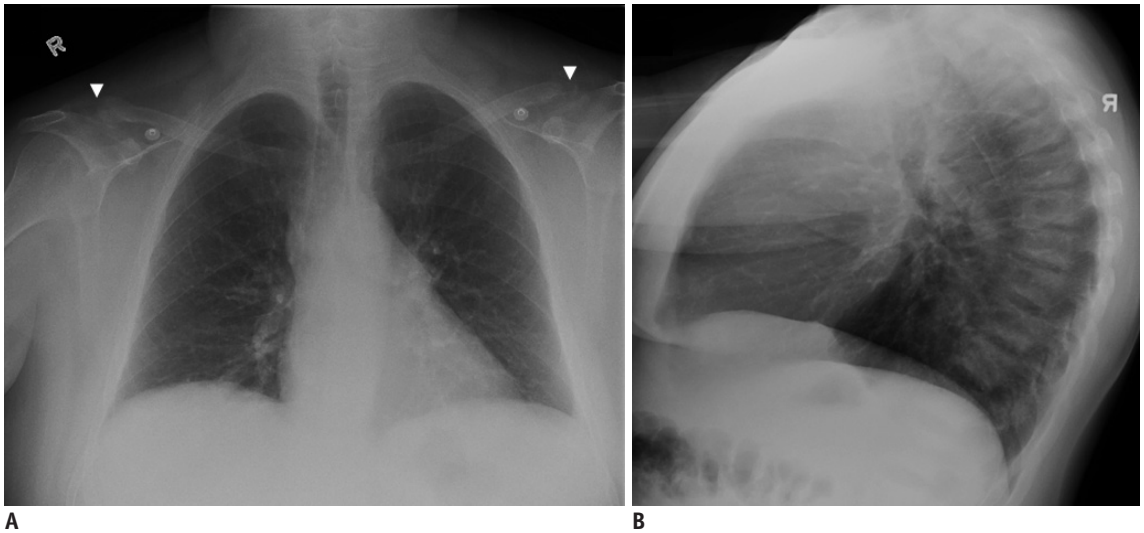

A B

Fig. 14. Hyperparathyroidism.
Frontal **(A)** and lateral **(B)** chest radiographs of 31-year-old male with secondary hyperparathyroidism due to chronic renal failure show resorption of distal clavicles (arrowheads) and "rugger-jersey" spine.

https://doi.org/10.3348/kjr.2019.0181

Korean Journal of Radiology
KJR

"rachitic rosary," referring to nodular enlargement of the costochondral junctions that can be apparent both clinically and radiologically (Fig. 15). Other radiological features of rickets include widening of the growth plates, metaphyseal flaring, cupping and fraying (Fig. 15), generalized osteopenia, bone deformities, especially bowing of legs, and insufficiency fractures (13).

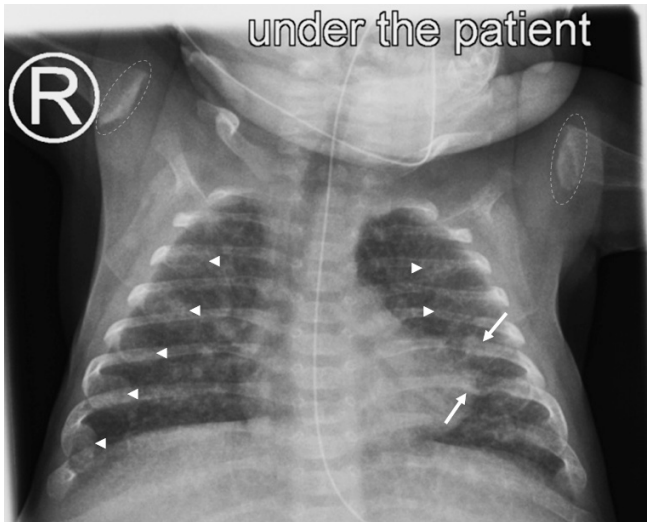

Fig. 15. Rickets. Frontal chest radiograph of 3-month-old premature-born female with rickets demonstrates healing fractures of left posterior 6th and 7th ribs (arrows), nodular widening of bilateral costochondral junctions–rachitic rosary (arrowheads) and fraying of proximal humeral metaphyses (dashed outlines).

Sickle Cell Anemia

Sickle cell anemia is an autosomal recessive genetic disorder characterized by abnormally shaped (sickled) red blood cells (RBCs). The underlying abnormality is the presence of abnormal hemoglobin, which, when deoxygenated, becomes relatively insoluble and forms long aggregates, which distort the RBC. The sickled RBCs cause vascular occlusion, which leads to tissue ischemia and infarction (14). Chest imaging usually reveals cardiomegaly and cephalization of pulmonary vessels due to a chronic high cardiac output state. H-shaped vertebrae and occasional avascular necrosis of humeral heads are almost pathognomonic for this condition (Fig. 16).

Thalassemia

RBCs are normally produced in the bone marrow. In cases of chronic anemia, where RBC production by bone marrow is not sufficient, hematopoiesis may extend beyond the confinement of the cortical bone that commonly occurs in the chest (15). Most cases of extramedullary hematopoiesis (EMH) are observed in patients with thalassemia. EMH typically appears as a posterior mediastinal abnormality, in the form of well-defined smooth or lobulated bilateral oblong paravertebral masses (Fig. 17). CT may also reveal osseous changes of chronic anemia in the form of bone expansion and coarsened trabeculations (Fig. 17). MRI may

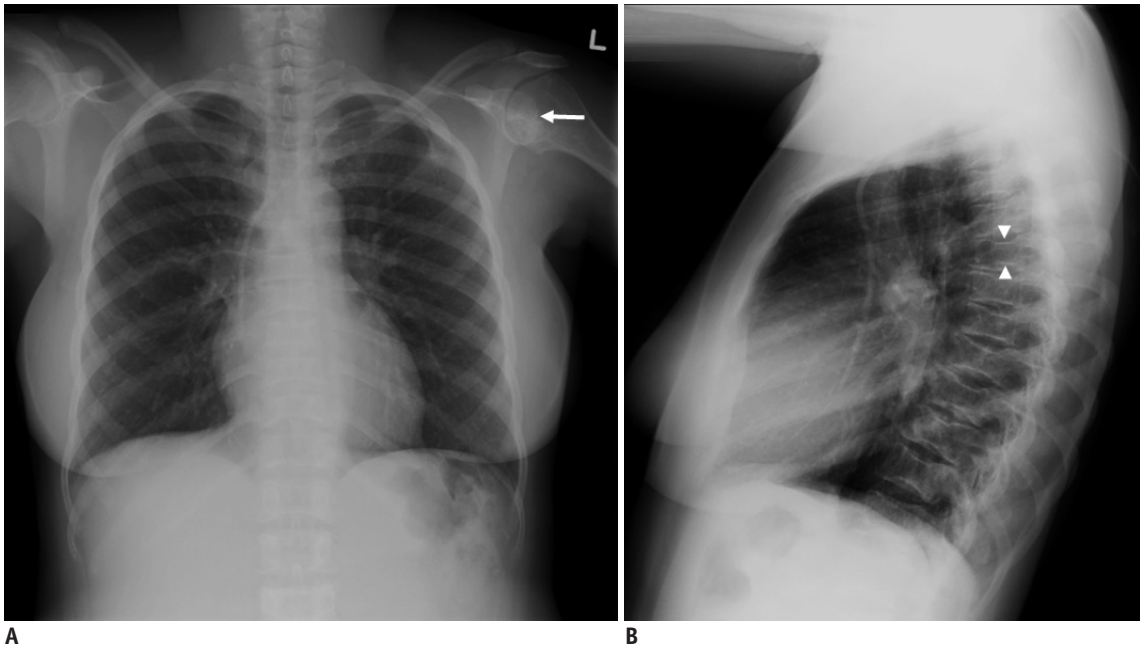

A B

Fig. 16. Sickle cell anemia.
Frontal **(A)** and lateral **(B)** chest radiographs of 39-year-old female with sickle cell anemia demonstrate H-shaped vertebrae (arrowheads) and left humeral head subchondral sclerosis (arrow), consistent with avascular necrosis.

https://doi.org/10.3348/kjr.2019.0181

show low signal intensity of the bone marrow, denoting active red marrow and iron deposition (Fig. 18).

Tuberculosis

Tuberculosis (TB) results from infection by *mycobacterium tuberculosis* and several other mycobacterial species. MSK involvement with TB is relatively uncommon and is reported in 1–3% of cases (16). The thoracic and lumbar spines are most frequently involved, referred to as the so-called Pott's disease. Infection usually begins in the anterior part of the vertebral body adjacent to the end plate and then spreads to the intervertebral disk, with subsequent dissemination into additional spinal segments and paraspinal tissues, resulting in the formation of a paravertebral abscess (Fig. 19). The untreated infection may eventually result in vertebral collapse and anterior wedging, leading to kyphosis and gibbus formation. TB spondylitis is characteristically associated with little or no reactive sclerosis or local periosteal reaction, a feature that helps distinguish it from pyogenic spondylitis (16).

Septic Arthritis of the Sternoclavicular Joint

Staphylococcus aureus is responsible for almost half of the cases of septic arthritis of sternoclavicular joint. Common risk factors include intravenous drug use, distant site of infection, diabetes mellitus, trauma, and infected central venous line (17). Plain radiography may show sclerosis of the medial clavicle and manubrium. The earliest findings seen on CT or MRI are joint effusion, widening of the joint space, or mild cortical irregularity. Osteomyelitis of the distal clavicle, the manubrium, or both, seen as bony erosions or sclerosis on CT (Fig. 20), and bone marrow edema on MRI, may be present in up to 55% of cases. Chest wall abscess or phlegmon (Fig. 20) and mediastinitis are common.

Elastofibroma Dorsi

Elastofibroma dorsi is fibroelastic pseudotumor thought to result from repeated mechanical friction between the chest wall and the tip of the scapula (18). Patients often have an occupational history of manual labor, such as farming. Most patients are older adults. Most elastofibromas are clinically occult. The most common symptom is stiffness, which is observed in approximately one-fourth of the patients (18). The location between the chest wall and inferior scapular tip is most characteristic of elastofibroma. Bilateral lesions are seen in up to 66% of cases. On CT, elastofibroma presents as a poorly defined, inhomogeneous soft-tissue density with attenuation similar to that of skeletal muscle

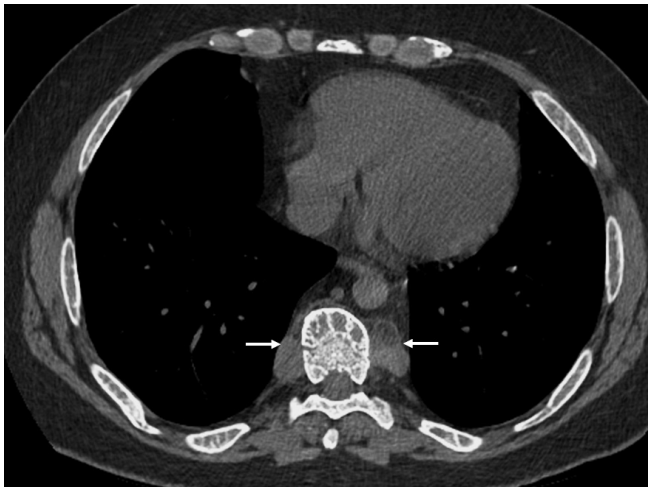

Fig. 17. Beta thalassemia. Chest CT scan of 44-year-old male with beta thalassemia intermedia shows diffuse expansion of osseous medullary spaces, coarsened trabeculations of ribs and vertebrae, and paravertebral extramedullary hematopoiesis (arrows).

Fig. 18. Beta thalassemia. Sagittal T1-weighted MRI of spine in 9-year-old male with beta thalassemia major shows diffuse abnormally low signal intensity of bone marrow related to active red marrow and iron deposition from multiple blood transfusions. Note that bone marrow (asterisk) is of significantly lower intensity than intervertebral disks (arrowhead).

https://doi.org/10.3348/kjr.2019.0181

Korean Journal of Radiology
KJR

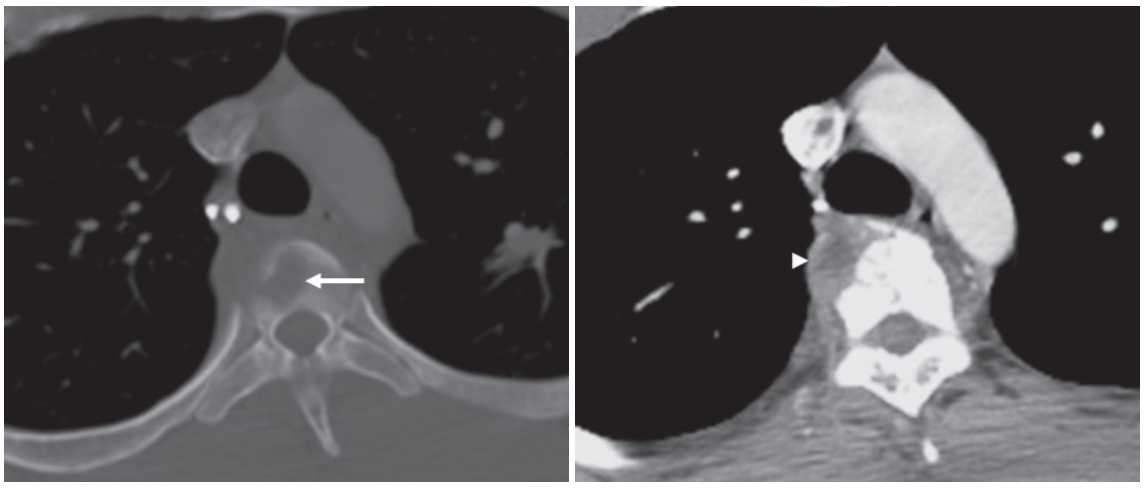

A B

Fig. 19. Tuberculosis.
Chest CT in bone **(A)** and mediastinal **(B)** windows of 23-year-old male with active post-primary pulmonary tuberculosis and spondylitis demonstrates irregular lytic lesion involving superior endplate of dorsal vertebra (arrow) and associated perivertebral abscess (arrowhead).

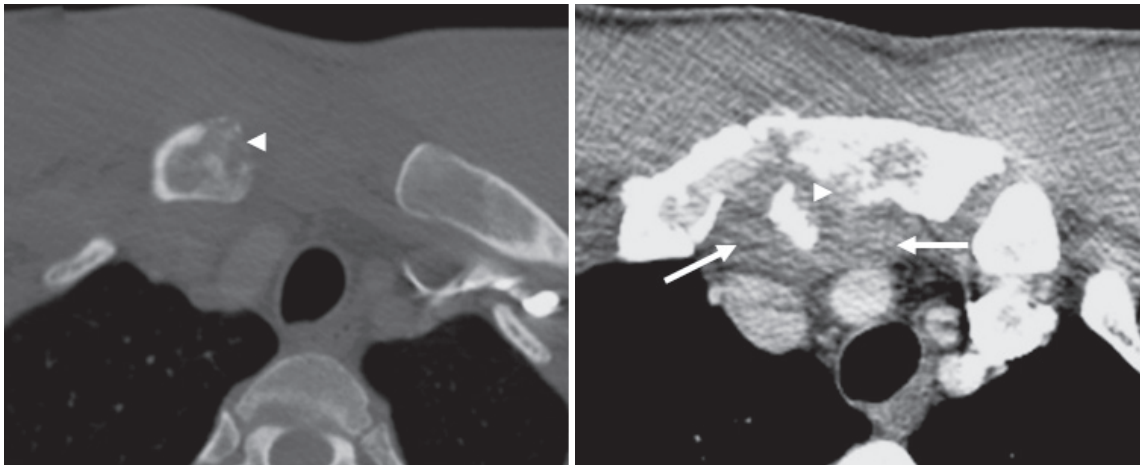

A B

Fig. 20. Septic arthritis of sternoclavicular joint.
Chest CT in bone **(A)** and mediastinal **(B)** windows of 41-year-old male, who developed septic arthritis of right sternoclavicular joint several weeks following penetrating injury to chest, demonstrates erosive lesions in right clavicular head and manubrium (arrowheads) consistent with osteomyelitis, and adjacent phlegmonous collection (arrows).

and containing linear low-density streaks (Fig. 21). On both T1- and T2-weighted images, the lesion appears as a well-defined lenticular mass with intermediate signal intensity approximately equal to that of skeletal muscle, with interlaced areas of high signal intensity similar to that of fat.

Sternal Dehiscence

Sternal dehiscence (SD) refers to disruption of the sternotomy fixation. When SD occurs in the first post-operative weeks, it is usually secondary to an off-center sternotomy or faulty sternal wires (19). SD two weeks after surgery is typically associated with sternal osteomyelitis

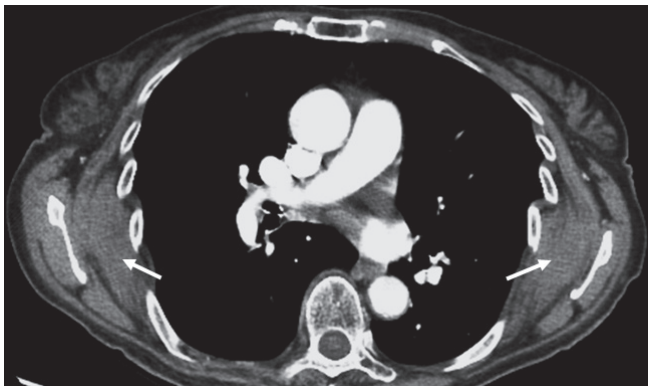

Fig. 21. Elastofibroma dorsi. Chest CT scan of 81-year-old female shows bilateral soft-tissue masses between scapulae and rib cage (arrows), consistent with bilateral elastofibroma dorsi.

https://doi.org/10.3348/kjr.2019.0181

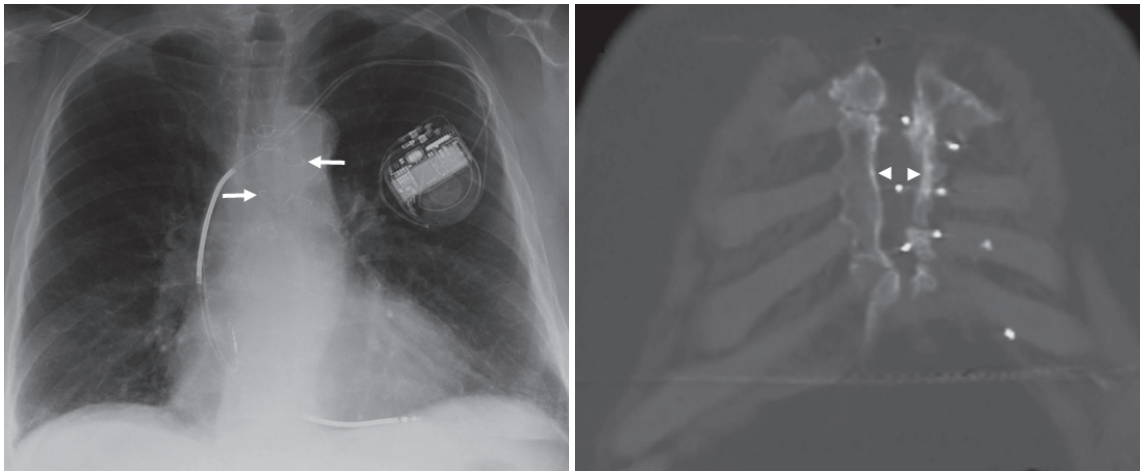

A B

Fig. 22. Sternal dehiscence. 72-year-old male with chronic sternal dehiscence following remote median sternotomy for aorto-coronary bypass surgery.
A. Chest radiograph shows fractures and misalignment of many sternal wires (arrows). **B.** Chest CT with coronal reformation shows separation of sternotomy edges (arrowheads).

and mediastinitis. Unrecognized SD may lead to osseous nonunion, which can cause severe pain. Progressive post-operative displacement, rotation, or fracture of the sternal wires on serial chest radiographs are all reliable signs of SD (Fig. 22). A more specific radiographic sign of SD is the presence of a lucent strip of more than 3 mm in width along the sternotomy. CT may show signs of underlying sternal osteomyelitis and/or mediastinitis.

SUMMARY

This pictorial essay illustrates the importance of recognition of certain chest wall abnormalities on imaging, as it can facilitate accurate diagnosis of several associated syndromes and other pathological conditions.

Conflicts of Interest

The authors have no potential conflicts of interest to disclose.

ORCID iDs

Alexandre Semionov
https://orcid.org/0000-0002-8255-3324
John Kosiuk
https://orcid.org/0000-0003-2643-8484
Amr Ajlan
https://orcid.org/0000-0001-8199-1915
Federico Discepola
https://orcid.org/0000-0002-8556-9153

REFERENCES

1. van Hoorn JH, Moonen RM, Huysentruyt CJ, van Heurn LW, Offermans JP, Mulder AL. Pentalogy of Cantrell: two patients and a review to determine prognostic factors for optimal approach. *Eur J Pediatr* 2008;167:29-35
2. Samartzis D, Herman J, Lubicky JP, Shen FH. Sprengel's deformity in Klippel-Feil syndrome. *Spine (Phila Pa 1976)* 2007;32:E512-E516
3. Paul SA, Simon SS, Karthik AK, Chacko RK, Savitha S. A review of clinical and radiological features of cleidocranial dysplasia with a report of two cases and a dental treatment protocol. *J Pharm Bioallied Sci* 2015;7(Suppl 2):S428-S432
4. Urschel HC Jr. Poland syndrome. *Semin Thorac Cardiovasc Surg* 2009;21:89-94
5. Stark Z, Savarirayan R. Osteopetrosis. *Orphanet J Rare Dis* 2009;4:5
6. Fortman BJ, Kuszyk BS, Urban BA, Fishman EK. Neurofibromatosis type 1: a diagnostic mimicker at CT. *Radiographics* 2001;21:601-612
7. Ha HI, Seo JB, Lee SH, Kang JW, Goo HW, Lim TH, et al. Imaging of Marfan syndrome: multisystemic manifestations. *Radiographics* 2007;27:989-1004
8. Newman CA, Reuther WL 3rd, Wakabayashi MN, Payette MM, Plavsic BM. Gastrointestinal case of the day. Gardner syndrome. *Radiographics* 1999;19:546-548
9. Capobianco J, Grimberg A, Thompson BM, Antunes VB, Jasinowodolinski D, Meirelles GS. Thoracic manifestations of collagen vascular diseases. *Radiographics* 2012;32:33-50
10. Johnson TH, Mital N, Rodnan GP, Wilson RJ. Relapsing polychondritis. *Radiology* 1973;106:313-315
11. Wang YF, Teng MM, Chang CY, Wu HT, Wang ST. Imaging manifestations of spinal fractures in ankylosing spondylitis. *AJNR Am J Neuroradiol* 2005;26:2067-2076

https://doi.org/10.3348/kjr.2019.0181

12. Duncan JG. Radiological manifestations of hyperparathyroidism. *Proc R Soc Med* 1956;49:283-286
13. Calder AD. Radiology of osteogenesis imperfecta, rickets and other bony fragility states. *Endocr Dev* 2015;28:56-71
14. Lonergan GJ, Cline DB, Abbondanzo SL. Sickle cell anemia. *Radiographics* 2001;21:971-994
15. Haidar R, Mhaidli H, Taher AT. Paraspinal extramedullary hematopoiesis in patients with thalassemia intermedia. *Eur Spine J* 2010;19:871-878
16. Burrill J, Williams CJ, Bain G, Conder G, Hine AL, Misra RR. Tuberculosis: a radiologic review. *Radiographics* 2007;27:1255-1273
17. Ross JJ, Shamsuddin H. Sternoclavicular septic arthritis: review of 180 cases. *Medicine (Baltimore)* 2004;83:139-148
18. Kransdorf MJ, Meis JM, Montgomery E. Elastofibroma: MR and CT appearance with radiologic-pathologic correlation. *AJR Am J Roentgenol* 1992;159:575-579
19. Restrepo CS, Martinez S, Lemos DF, Washington L, McAdams HP, Vargas D, et al. Imaging appearances of the sternum and sternoclavicular joints. *Radiographics* 2009;29:839-859

 https://doi.org/10.3348/kjr.2019.0181